# Electrode polarization and charge transport at solid interfaces

A. Serghei,[1,2,*] M. Tress,[1] J. R. Sangoro,[1] and F. Kremer[1]
[1]*Institute for Experimental Physics I, University of Leipzig, 04103 Leipzig, Germany*
[2]*Department of Polymer Science and Engineering, University of Massachusetts Amherst, Amherst, Massachusetts 01003, USA*
(Received 4 October 2009; published 5 November 2009)

A quantitative description is suggested for electrode polarization, an ubiquitous phenomenon which takes place at the interface between a metallic and an ionic conductor and results in an increase by many orders of magnitude in the net dielectric response of the sample cell. Based on the fact that due to coulombic interactions, the mobility of charge carriers is drastically slowed down at the metal/ionic conductor interface, this approach quantitatively reproduces the observed scaling laws and opens perspectives in the physics of charge transport at interfaces.

DOI: 10.1103/PhysRevB.80.184301 PACS number(s): 66.10.Ed, 82.45.Fk

## I. INTRODUCTION

Electrode polarization is an ubiquitous phenomenon taking place at the interface between a metallic and an ionic conductor. It shows a characteristic signature in the net dielectric response of the sample cell in dependence on frequency of the applied electric field, temperature, concentration of the charge carriers, and the sample length.[1–20] Furthermore, it is well known that electrode polarization is strongly affected by the material of the electrodes, a finding which lacks—until now—a microscopic understanding.

In this paper a quantitative description of the electrode polarization is suggested by taking into consideration the mechanism of charge transport at interfaces. This approach reproduces unambiguously the observed scaling laws[5] and opens perspectives in the physics of charge transport at solid interfaces.

## II. MATERIALS AND METHODS

Several ionic liquids (purchased from Solvent Innovation GmbH and Iolitec GmbH) are investigated in the current work: 1-Hexyl-3-methylimidazolium chloride, 1-Hexyl-3-methylimidazolium hexafluorophosphate (HMIM-$PF_6$), 1,3-dimethylimidazolium dimethylphosphate (MMIM-$Me_2PO_4$), trioctylmethylammonium bis(trifluoromethylsulfonyl)imide. Sodium chloride solutions of different concentrations (in millipore water) are examined, as well. The dielectric measurements are carried out using a high resolution alpha analyzer (Novocontrol GmbH) and a HP impedance analyzer, both assisted by Quatro temperature controllers. The samples are measured in a parallel-plate geometry, using circular metallic plates of 20 mm diameter as electrodes and small flat Teflon pieces as spacers (having a well-controlled thickness on the submillimeter length scale). The applied voltages (always chosen in the linear regime) are on the order of 0.1–0.2 V.

## III. ELECTRODE POLARIZATION: EXPERIMENTAL FEATURES

The typical signature in the frequency and temperature dependence of the complex permittivity $\varepsilon^*=\varepsilon'-i\varepsilon''$ and conductivity $\sigma^*=\sigma'+i\sigma''$ of ionic liquids is shown in Fig. 1. At high frequencies (and low temperatures) the dielectric response is dominated by charge transport processes in the bulk. This contribution is reflecting well-defined molecular physical quantities (as, for instance, the hopping time and the effective number density of the charge carriers) and is described by recent models of charge transport in disordered systems.[21,22] At lower frequencies (and high temperatures) changes by many orders of magnitude in the measured values of $\varepsilon^*$ or $\sigma^*$ are detected due to electrode polarization effects. It is important to notice that these values (as for instance $\varepsilon' \cong 10^6$) do not have any longer a direct molecular interpretation (as for the bulk) but reflect the net impedance of the measured cell, where the contribution of the interfaces must be added to that of the bulk. Given the fact that in the majority of the studies investigating the mechanisms of charge transport the experimental data are represented in terms of $\varepsilon^*$ or $\sigma^*$, we adopt in this paper the same representation to discuss our model.

The most prominent features of electrode polarization, as manifested in measurements of $\varepsilon^*$ or $\sigma^*$, are emphasized by arrows in Fig. 1 (for a particular temperature of 240 K). These effects are coming into play at a certain frequency $f_{on}$ ("onset of the electrode polarization"), where a steep increase in $\varepsilon'$ (corresponding to a minimum in $\sigma''$) is detected first. At lower frequencies ($f \approx f_{max}$, "full development of the electrode polarization"), a plateau in $\varepsilon'$ starts to develop, corresponding to a peak in $\sigma''$. At the same frequency $f \approx f_{max}$ the real part of the conductivity $\sigma'$ begins to decrease while a peak in $\varepsilon''$ shows up. Despite these peculiar frequency dependencies, a perfect scaling is observed in both $\sigma'$ and $\sigma''$ (or, correspondingly, in $\varepsilon'$ and $\varepsilon''$) upon varying the temperature: all measured experimental curves collapse onto a single chart when normalized. This finding can be expressed more comprehensible by plotting together $f_{max}$, $f_{on}$, and $\sigma_0$ (the dc conductivity) as a function of inverse temperature. Parallel Vogel-Fulcher-Tamann-type temperature dependences are obtained,[23] implying—in a frequency range covering many orders of magnitude—the simple relation

$$f_{max} \sim f_{on} \sim \sigma_0. \quad (1)$$

Further parameters influencing the dielectric measurements in the low-frequency region are systematically examined in

 

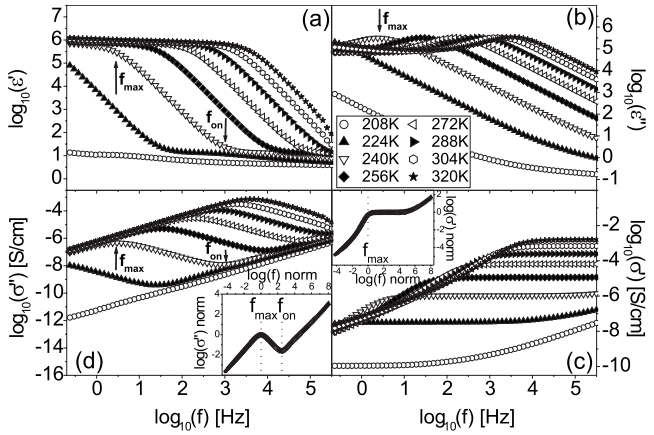


FIG. 1. Complex dielectric permittivity $\varepsilon^*=\varepsilon'-i\varepsilon''$ and conductivity $\sigma^*=\sigma'+i\sigma''$ of HMIM-$PF_6$ versus frequency at different temperatures, as indicated. The arrows mark, for a particular temperature of 240 K, the frequencies $f_{on}$ (onset of electrode polarization) and $f_{max}$ (full development of electrode polarization). In the insets, $\sigma'$ [Fig. 1(c)] and $\sigma''$ [Fig. 1(d)] are presented normalized with respect to the peak position. All logarithms are in the decimal base.

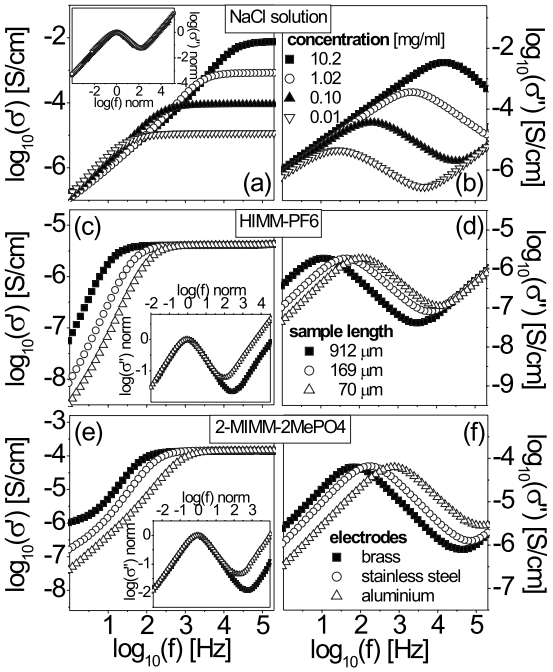


FIG. 2. $\sigma'$ and $\sigma''$ versus frequency showing the dependence of electrode polarization effects on: [(a) and (b)] concentration of the charge carriers (for NaCl solutions); [(c) and (d)] length of the sample cell (for HMIM-$PF_6$); and [(e) and (f)] material of the electrodes (for MMIM-$Me_2PO_4$). In the insets, the curves of $\sigma''$ versus frequency are presented normalized with respect to the peak position. All logarithms are in the decimal base.

Fig. 2. A concentration dependence is analyzed by measuring different NaCl solutions [Figs. 2(a) and 2(b)]. The position of $f_{on}$ and $f_{max}$ is shifted to higher frequencies when the concentration increases. Similarly to the temperature dependence, the dielectric and conductivity measurements scale with respect to variation in the concentration, i.e., collapsing normalized curves are obtained [inset Fig. 2(a)]. By replotting $f_{max}$ and $f_{on}$ as a function of $\sigma_0$, a scaling law identical to that given by Eq. (1) is found.[23]

Changing the length $L$ of the sample cell causes pronounced alterations of the dielectric response in the low-frequency region. A systematic dependence is discussed in Figs. 2(c) and 2(d). Decreasing the sample length shifts the position of $f_{on}$ and $f_{max}$ to higher frequencies. In contrast to the temperature or concentration dependence, *no* scaling with respect to variation of sample length is found [inset Fig. 2(c)]. This implies different scaling laws for $f_{on}$ and $f_{max}$ as a function of $L$. Indeed, $f_{max} \sim 1/L^{1.0\pm0.1}$ while $f_{on} \sim 1/L^{0.5\pm0.1}$ is determined from the experimental data.[23]

Another important parameter influencing the phenomenon of electrode polarization represents the material of the electrodes. This is exemplified in Figs. 2(e) and 2(f) showing dielectric measurements carried out using various materials for the electrodes (while keeping constant the other parameters characterizing the sample cell, i.e., length, area, roughness, applied voltage, etc…). Pronounced changes in the dielectric spectra are found, which, similarly to the situation when the length dependence was investigated, do not exhibit scaling.

## IV. ELECTRODE POLARIZATION: THEORETICAL MODEL

The experimental findings described in Figs. 1 and 2 can be fully understood by analyzing the hopping process of the charge carriers in the (nanometric) vicinity of the metal/ionic conductor interface. Basic considerations of electrochemistry[24] evidence the fact that due to the strong coulombic forces between the ions and the charged metallic electrodes upon applying a voltage across the sample cell, interaction energies $\Delta E_c$ larger than the thermal energy $k_BT$ are reached ($\Delta E_c \gg k_BT$). Being well known[22] that the hopping time of the charge carriers $\tau_e$ depends exponentially on the activation energy $E$

$$\tau_e = \tau_0 \exp\left(\frac{E}{k_BT}\right), \tag{2}$$

where $\tau_0$ is a constant, the Coulombic interactions manifested at the metallic interfaces will lead to a tremendous increase in the hopping time

$$\frac{\tau_e(\text{interface})}{\tau_e(\text{bulk})} \cong \exp\left(\frac{\Delta E_c}{k_BT}\right) \gg 1. \tag{3}$$

This will result in a correspondingly large decrease in the values of dc conductivity $\sigma_0$ at the interface

$$\frac{\sigma_0(\text{bulk})}{\sigma_0(\text{interface})} \gg 1 \tag{4}$$

since $\sigma_0 \sim \frac{1}{\tau_e}$, relation (known as the Barton-Nakajima-Namikawa relation) which can be directly derived by considering the Einstein and Einstein-Smolochowski equations.[25]

The measured complex permittivity $\varepsilon^*_{\text{meas}}$ can be calculated by taking into account the dielectric function of the ionic liquid in the bulk $\varepsilon^*_b=\varepsilon'_b-i\varepsilon''_b$ and that of the ionic liquid at the interface $\varepsilon^*_i=\varepsilon'_i-i\varepsilon''_i$

$$\frac{L}{\varepsilon^*_{\text{meas}}}=\frac{2d_i}{\varepsilon^*_i}+\frac{L-2d_i}{\varepsilon^*_b}, \tag{5}$$

where $L$ is the length of the sample cell and $d_i$ the thickness of the interfacial regions. For the bulk, analytical functions derived in a recently developed microscopic model of the charge transport in disordered systems are employed[22]

$$\sigma^*(\omega)=\sigma_0\left[\frac{i\omega\tau_e}{\ln(1+i\omega\tau_e)}\right] \tag{6}$$

together with $\varepsilon^*=\frac{\sigma^*}{i\varepsilon_0\omega}$.

For the interfacial regions (having thicknesses on the length scale defined by the screening length of the Coulombic interactions, i.e., ~1 nanometer), a formula similar to Eq. (6) is used, but, in accord to Eqs. (3) and (4), the following condition is imposed:

$$\frac{\tau_e(\text{interface})}{\tau_e(\text{bulk})}\cong\frac{\sigma_0(\text{bulk})}{\sigma_0(\text{interface})}\gg 1. \tag{7}$$

It is important to mention at this point that while relation (7) has a solid physical justification (2,3,4), Eq. (6) was developed to express the conductivity of ion conductive materials in the *bulk*. Its applicability to describe the interfacial charge hopping mechanism is limited but justified by the fact that *no* explicit theoretical developments aiming to deliver conductivity (or permittivity) functions at the interfaces exist at present in the literature. Additionally, it can be easily shown that other approaches used to describe the conductivity in the bulk (as for instance the universal model of Jonscher[26]) can be alternatively employed with similar conclusions on the electrode polarization effects, as long as condition (7) is imposed.

Given the fact that the current density $\vec{j}=\sigma^*\vec{E}$ is constant across the length of the sample cell, changes in the conductivity function at the interface will automatically imply redistributions of the local-field strengths. In our particular case, the conductivity decreases leading to an increase in the strength of the local electric field $E$ of the interfacial regions.

The calculations of the complex permittivity and conductivity according to Eq. (5), are shown in Fig. 3 (interfacial regions of 1 nm thickness are assumed). In a wide frequency range covering about 10 orders of magnitude, the spectral dependence of the electrode polarization effects (leading to changes by about 6 orders of magnitude in the intensity of the measured dielectric responses) is *quantitatively* reproduced. This approach, successful to describe in detail the frequency dependence of the experimentally determined $\varepsilon^*$ and $\sigma^*$, can be approximated to a simpler form, suitable to treat analytically two important aspects related to the electrode polarization effects: (a) the scaling laws in respect to the variation in temperature, concentration, length of the sample cell, and material of the electrodes,[5] (b) the influence of intermediate "transition" regions (between the interface and the bulk), where the local dielectric properties are supposed to gradually vary from the interfacial to the bulk region.

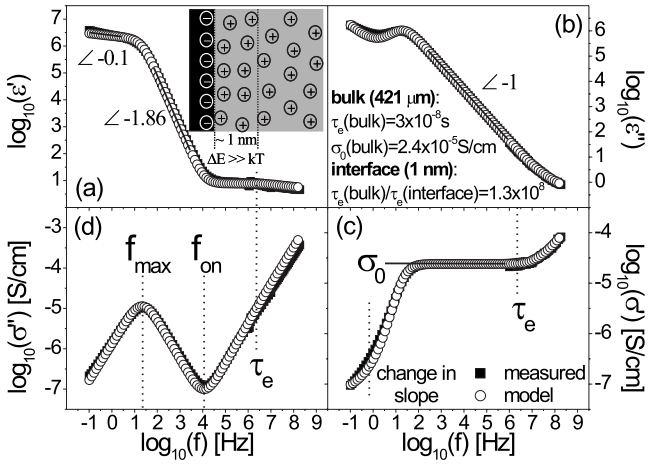


FIG. 3. Measured and calculated (Eqs. (5)–(7)) complex dielectric permittivity $\varepsilon^*=\varepsilon'-i\varepsilon''$ and conductivity $\sigma^*=\sigma'+i\sigma''$ of HMIM-$PF_6$ versus frequency at 264 K. In addition to the bulk contribution, interfacial regions of 1 nm thickness were assumed in the calculations with $\frac{\tau_e(\text{interface})}{\tau_e(\text{bulk})}=\frac{\sigma_0(\text{bulk})}{\sigma_0(\text{interface})}=1.3\times10^8$. In the panel 3a only the positive ions are shown, for simplicity. All logarithms are in the decimal base.

Since $\frac{\tau_e(\text{interface})}{\tau_e(\text{bulk})}\cong\frac{\sigma_0(\text{bulk})}{\sigma_0(\text{interface})}\gg1$, it follows immediately that $\frac{\varepsilon''(\text{interface})}{\varepsilon''(\text{bulk})}\ll1$. This relation can be approximated by setting $\varepsilon''(\text{interface})\cong0$. The results are shown in Fig. 4. Except small deviations detectable in the low-frequency side of the spectra ($f\ll f_{\max}$), the onset as well as the full development of electrode polarization effects are correctly recovered. It can be easily demonstrated that $\varepsilon''(\text{interface})\to0$ would imply a measured phase angle (between the applied voltage and the resulting current) approaching a value of −90° in the low-frequency limit, which is indeed close to the experimental observation (−86°).

In addition to the interfacial regions [where $\varepsilon''(\text{interface})\to0$ is supposed for mathematical simplicity], transition regions where the local physical quantities gradually vary from the interface to the bulk can be taken into account. Instead of Eq. (5) one has to use

$$\frac{L/2}{\varepsilon^*_{\text{meas}}}=\frac{d_i}{\varepsilon^*_i}+\int_{di}^{L/2}\frac{dx}{\varepsilon^*(x)}, \tag{8}$$

where for $\varepsilon^*(x)$ an exponential decrease with a decay factor of $\kappa=1/d_D$ ($d_D$ being the effective thickness of the transition regions) is assumed between $x=L/2$ and $x=d_i$. The condition $\varepsilon''(\text{interface})\to0$ simplifies to a large extent the analytical calculations necessary to impose the Kramers-Kronig relation between $\varepsilon'(x)$ and $\varepsilon''(x)$, both exponentially decreasing at the interface. It is found that including a transition region exhibiting a gradual variation in $\varepsilon^*(x)$ does not lead to changes as compared to the situation when only the interfacial layers characterized by $\varepsilon^*_i$ are considered. On the other hand, taking into account only the exponential decay of $\varepsilon^*(x)$

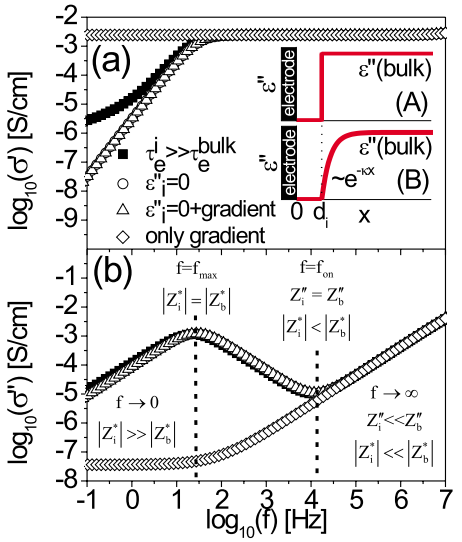


FIG. 4. (Color online) Calculated complex conductivity $\sigma^* = \sigma' + i\sigma''$ (according to Eq. (5)) assuming: (■) 1 nm thick interfacial regions with $\frac{\tau_e(\text{interface})}{\tau_e(\text{bulk})} = \frac{\sigma_0(\text{bulk})}{\sigma_0(\text{interface})} = 10^8$ and $\sigma^*(\text{interface})$ given by Eq. (6); (○) 1 nm interfacial regions with $\varepsilon''(\text{interface}) = 0$; (△) 1 nm interfacial regions with $\varepsilon''(\text{interface}) = 0$ and transition regions where $\varepsilon'$ and $\varepsilon''$ are exponentially varying between the interfacial and bulk values with a decay coefficient of $\kappa = 1$ nm$^{-1}$; (◇) only transition regions where $\varepsilon'$ and $\varepsilon''$ are exponentially varying between the interfacial and bulk values with a decay coefficient of $\kappa = 1$ nm$^{-1}$. Panels: (4a) gradients in the local dielectric properties are schematically illustrated; (4b) the physical significance of $f_{on}$ and $f_{max}$, expressed in terms of bulk and interfacial impedances. All logarithms are in the decimal base.

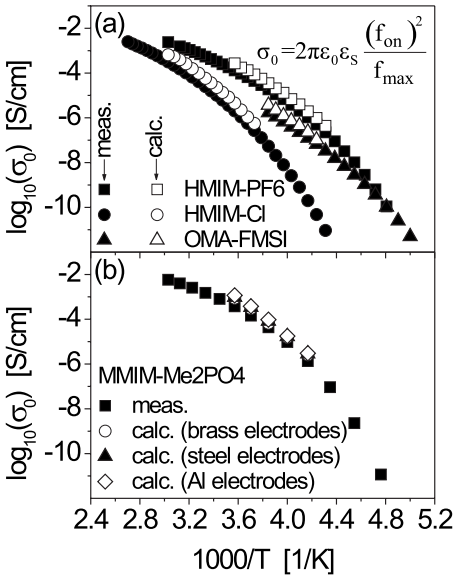


FIG. 5. (a) Measured and calculated ($\sigma_0 = 2\pi\varepsilon_0\varepsilon_S \frac{(f_{on})^2}{f_{max}}$) dc conductivities for a variety of ionic liquids; (b) dc conductivities calculated from the measurements shown in Figs. 2(e) and 2(f) for various electrode materials. Despite strongly different values of $f_{max}$ and $f_{on}$, the calculated dc conductivities are in full agreement with the direct measurements. All logarithms are in the decimal base.

at the interface without the interfacial layers does not lead to curves reproducing the spectral features of the electrode polarization effects. These considerations clearly show that the low-frequency side of the dielectric curves (in the region where $f \ll f_{max}$) is dominated by the charge transport mechanisms in the interfacial regions.

The approximation $\varepsilon''(\text{interface}) \to 0$ allows one to examine the scaling laws of the electrode polarization[5] by finding the analytical solutions of the equation: $\frac{d}{d\omega}(\sigma''_{meas}) = 0$ and analyzing the resulting formula for $f_{on}$ and $f_{max}$ in dependence on $\sigma_0$, $L$, and $d_i$. Thus

$$f_{on} \cong \frac{\sigma_0}{\varepsilon_0} \frac{1}{2\pi\sqrt{\varepsilon'_b \varepsilon'_i}} \sqrt{\frac{2d_i}{L}} \quad \text{and} \quad f_{max} \cong \frac{\sigma_0}{\varepsilon_0} \frac{1}{2\pi\varepsilon'_i} \frac{2d_i}{L}, \quad (9)$$

where $\varepsilon'_b$ and $\varepsilon'_i$ are the dielectric permittivities of the material in the bulk and at the interface.

It is immediately obvious that (i) $f_{max} \sim f_{on} \sim \sigma_0$, which is identical to the scaling laws observed experimentally upon varying the temperature or the concentration of the charge carriers. (ii) $f_{on} \sim \frac{1}{\sqrt{L}}$, while $f_{max} \sim \frac{1}{L}$, in quantitative agreement with the measured values and with the experimental observation that the dielectric response does not scale with respect to the variation in the sample length. (iii) $f_{on} \sim \sqrt{d_i}$ while $f_{max} \sim d_i$ which delivers a qualitative explanation of the dependence on the material of the electrodes since varying the material of the electrodes is expected to change the thickness of the interfacial layers. In addition, possible effects arising due to differently thick oxide layers should be considered as well. Furthermore, the experimental observation that the dielectric response does not scale with respect with the variation in the electrode material is recovered, as well. (iv) $f \cong f_{max}$ is a solution for both $\frac{d}{d\omega}(\sigma''_{meas}) = 0$ and $\frac{d}{d\omega}(\varepsilon''_{meas}) = 0$ which explains the experimental finding that the peaks detected in $\sigma''_{meas}$ and $\varepsilon''_{meas}$ appear at the same frequency position. (v) $\sigma_0 = 2\pi\varepsilon_0\varepsilon_S \frac{(f_{on})^2}{f_{max}}$, which is proven in Fig. 5 to deliver the correct dc conductivities for a variety of ionic liquids using only parameters extracted from the electrode polarization effects (except $\varepsilon_S$ which is the static permittivity of the material in the bulk measured at $f > f_{on}$). Moreover, this formula holds even in the case when $f_{on}$ and $f_{max}$ strongly depend on the material of the electrodes [Figs. 2(e), 2(f), and 5(b)], which indicates that the current theoretical approach renders the correct explanation for the dependence on the material of the electrodes.

Under the assumption $\varepsilon''(\text{interface}) \to 0$ [which in terms of impedances leads to $Z'(\text{interface}) \to 0$] it can be readily shown that the onset of the electrode polarization, as given by Eq. (9), represents the frequency position at which $Z''(\text{interface}) \cong Z''(\text{bulk})$ while the full development corresponds to $|Z^*(\text{interface})| \cong |Z^*(\text{bulk})|$ [inset Fig. 4(b)].

## V. CONCLUSIONS

In conclusion, the charge transport mechanism at the ion-metal interfaces is analyzed in detail in relation to the dielectric signature of the electrode polarization. The proposed the-

oretical approach, proven to reproduce the well-known scaling laws,[5] opens perspectives in the physics of charge transport at solid interfaces as it allows one to determine, using the phenomenon of the electrode polarization, the permittivity function—and, thus, the conduction mechanisms—in the interfacial regions.[23]

*Corresponding author; serghei@polysci.umass.edu

[1] H. Sanabria and J. H. Miller, Phys. Rev. E **74**, 051505 (2006).
[2] Y. Feldman, R. Nigmatullin, E. Polygalov, and J. Texter, Phys. Rev. E **58**, 7561 (1998).
[3] G. Barbero and A. L. Alexe-Ionescu, Liq. Cryst. **32**, 943 (2005); M. Becchi, C. Avendano, A. Strigazzi, and G. Barbero, J. Phys. Chem. B **109**, 23444 (2005).
[4] R. J. Klein, S. Zhang, S. Dou, B. H. Jones, R. H. Colby, and J. Runt, J. Chem. Phys. **124**, 144903 (2006).
[5] J. R. Macdonald, Phys. Rev. **92**, 4 (1953).
[6] J. R. Macdonald, J. Phys.: Condens. Matter **17**, 4369 (2005).
[7] A. Sawada, K. Tarumi, and S. Naemura, Jpn. J. Appl. Phys. **38**, 1423 (1999).
[8] R. Coelho, J. Non-Cryst. Solids **131-133**, 1136 (1991).
[9] P. Kohn, K. Schröeter, and T. Thurn-Albrecht, Phys. Rev. Lett. **99**, 086104 (2007).
[10] *Impedance Spectroscopy*, edited by E. Barsoukov and J. R. Macdonald (Wiley, New York, 2005).
[11] H. Chang and G. Jaffe, J. Chem. Phys. **20**, 1071 (1952).
[12] J. B. Bates, Y. T. Chu, and W. T. Stribling, Phys. Rev. Lett. **60**, 627 (1988).
[13] F. Bordi, C. Cametti, and R. H. Colby, J. Phys.: Condens. Matter **16**, R1423 (2004).
[14] E. Yariv and I. Frankel, Phys. Rev. Lett. **89**, 266107 (2002).
[15] H. Helmholtz, Pogg. Ann. **89**, 211 (1853).
[16] G. Gouy, Comt. Rend. **149**, 654 (1909); J. Phys. **4**, 457 (1910).
[17] D. L. Chapman, Philos. Mag. **25**, 475 (1913).
[18] O. Stern, Z. Electrochem. **30**, 508 (1924).
[19] M. T. Alam, M. M. Islam, T. Okajima, and T. Ohsaka, J. Phys. Chem. C **112**, 16600 (2008).
[20] M. V. Fedorov and A. A. Kornyshev, J. Phys. Chem. **112**, 11868 (2008); A. A. Kornyshev, *ibid.* **111**, 5545 (2007).
[21] *Broadband Dielectric Spectroscopy*, edited by F. Kremer and A. Schönhals (Springer, Berlin, 2003).
[22] J. C. Dyre and T. B. Schroder, Phys. Rev. B **54**, 14884 (1996); Rev. Mod. Phys. **72**, 873 (2000); T. B. Schroder and J. C. Dyre, Phys. Rev. Lett. **84**, 310 (2000).
[23] A. Serghei, M. Tress, and F. Kremer (unpublished).
[24] G. Grundmeier and M. Stratmann, Annu. Rev. Mater. Res. **35**, 571 (2005).
[25] J. R. Sangoro, A. Serghei, S. Naumov, P. Galvosas, J. Kärger, C. Wespe, F. Bordusa, and F. Kremer, Phys. Rev. E **77**, 051202 (2008); J. Sangoro, C. Iacob, A. Serghei, S. Naumov, P. Galvosas, J. Kärger, C. Wespe, F. Bordusa, A. Stoppa, J. Hunger, R. Buchner, and F. Kremer, J. Chem. Phys. **128**, 214509 (2008).
[26] A. K. Jonscher, *Dielectric Relaxations in Solids* (Chelsea Dielectric, London, 1983); A. K. Jonscher, Nature (London) **267**, 673 (1977).